View Article Online
View Journal

Green Chemistry

Cutting-edge research for a greener sustainable future

Accepted Manuscript

This article can be cited before page numbers have been issued, to do this please use: H. Günan, M. Vorobii and U. Schwaneberg, *Green Chem.*, 2026, DOI: 10.1039/D6GC00733C.

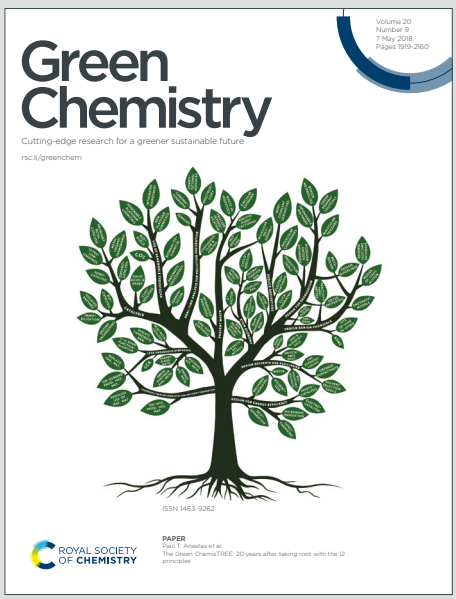

ROYAL SOCIETY OF CHEMISTRY

rsc.li/greenchem

View Article Online
DOI: 10.1039/D6GC00733C

Green Foundation

1. This work demonstrates a bio-based switchable adhesive system that enables both effective bonding during use and controlled debonding at the end of life, highlighting the potential of stimuli-responsive adhesion as a green processing strategy to address the recycling challenges associated with multilayer pharmaceutical blister packaging.
2. A bio-based adhesive composed of cellulose nanocrystals, chitosan and a bifunctional fusion protein was developed, enabling material-specific debonding under mild pH conditions or cellulase treatment. This approach avoids harsh solvents and high-energy activation, while facilitating selective separation of aluminum and plastic layers.
3. Future studies could optimize debonding conditions for industrial recycling, extend the concept to other multilayer material systems and incorporate quantitative life-cycle assessment for large-scale applications.

pH- and cellulase-triggered debonding of a bio-based adhesive designed to facilitate pharmaceutical blister pack recycling

View Article Online
DOI: 10.1039/D6GC00733C

Hande Günan[1,2], Mariia Vorobii[1], Ulrich Schwaneberg[1*]

[1] *Institute of Biotechnology, RWTH Aachen University, 52074, Aachen, Germany*

[2] *Department of Chemical Engineering, Hacettepe University, 06800, Ankara, Türkiye*

Abstract

Recycling pharmaceutical blister packaging waste remains a major challenge due to its complex multilayer structure. Here, a biodegradable adhesive design is proposed to address this issue, aiming to facilitate the separation of composite layers and promote sustainable recycling. The blend of cellulose nanocrystals (CNC) and chitosan (CH) at equal masses showed the highest bond strength after drying, confirming its efficiency as a glue matrix. The CBM3 domain (Carbohydrate-Binding Module Family 3) was genetically fused to the adhesion-promoting peptide Snakin-1 (also referred to as an anchor peptide), which exhibited binding affinity toward synthetic polymers used in blister packaging (Polyvinyl chloride (PVC) and PVC-based commercial products), as well as to aluminum layers. In fusion protein CBM3-Snakin1, a flexible Gly/Ala-rich linker provided spatial separation between the two domains, enabling their bifunctional binding behavior. Upon application between the target aluminum and plastic surfaces, the CNC/CH polysaccharide matrix containing the fusion protein showed approximately twofold higher binding strength compared to the protein-free matrix, reaching 98.5 kPa. Chemical characterization revealed new hydrogen bonding interactions between CNC, CH and CBM3-Snakin-1. Thermal analyses indicated that CNC increased the thermal stability of the CH matrix, while incorporation of the CBM3-Snakin-1 fusion protein limited chain mobility without adversely affecting thermal stability. Controlled, rapid and material-specific debonding was observed under both pH variations and cellulase treatments. The developed fully bio-based adhesive, composed of a CNC/CH polysaccharide matrix incorporating a CBM3-Snakin-1 fusion protein, achieved a sufficient binding strength and demonstrated on-demand delamination, providing a new perspective for pharmaceutical blister pack recycling.

Keywords: Blister packaging, stimuli-responsive adhesive, nanocellulose crystals (CNC), chitosan, anchor peptide, adhesion promoting peptide

* Corresponding author
Phone: +49 241 80-24176
E-mail: u.schwaneberg@biotec.rwth-aachen.de

View Article Online
DOI: 10.1039/D6GC00733C

1. Introduction

White pollution, which is caused by the huge amounts of plastic accumulation in nature, is a crucial issue posing a significant threat to the ecosystem[1]. Recent studies revealed the presence of micro and nano plastics in soil, freshwater and even ice cores, which led to taking those particles in the human body through inhalation and food.[2,3] Although landfilling and incineration remain the most widely used methods because of their time and cost advantages, the disposal of about 23 million tons of plastic waste each year and the toxic gases released during incineration highlight the need to increase recycling rates.[4] However, recycling targets still remain unmet mainly, because composite materials require the separation of their individual components, which is a complex and costly process.[5]

Management of the pharmaceutical blister packaging wastes has turned into a major challenge in terms of the circular economy issue recently. Those wastes are typically composed of aluminum foil, paper and/or plastic sheets. Polyvinyl chloride (PVC) is the primary plastic used in pharmaceutical packaging; but it may be laminated with polyvinylidene dichloride (PVDC), polychlorotrifluoroethylene (PCTFE) or cyclic olefin copolymer (COC) to enhance its mechanical and physical performance.[6] The widespread use of these products, driven by their convenience and their ability to effectively protect pharmaceuticals from moisture and oxygen, leads to the generation of large amounts of waste (i.e. almost 4% of daily packaging waste by weight).[7] Due to the poor adhesion of conventional non-reactive polymer glues on chemically inert substrates, reactive formulations (such as epoxy- or urethane-based adhesives) are strongly preferred for this application, as they interact with both polar plastic surfaces and metallic aluminum layers, resulting in strong interfacial bonding and thereby ensuring stable sealing performance during storage and handling.[8,9] Accordingly, the product safety critically depends on achieving sufficient binding strength to ensure package integrity throughout handling, storage and use, as required by pharmaceutical packaging standards.

Recycling pharmaceutical blister package waste remains highly challenging due to its multilayer composition and the strong interfacial adhesion between plastic and aluminum layers.[10] Most conventional separation methods are mainly based on solvent-based delamination enabling almost complete aluminum recovery under ideal conditions, though plastic residues typically remain adhered to the foil.[7] This contamination limits its suitability for high-quality recycling applications, since impurities not only reduce corrosion resistance of recycled aluminum, but also adversely affect its mechanical integrity.[11,12] Impurities in plastics including additives, coating residues and cross-contamination with other polymers create heterogeneity that hinders efficient recycling and reduces mechanical performance.[13] Studies

View Article Online
DOI: 10.1039/D6GC00733C

show that a high level of purity is crucial for both the technical performance and the market acceptance of recycled plastics in high-value applications.[14-16]

Switchable glues are recognized as an important technology for designing highly recyclable products, thereby facilitating the circular economy. These adhesives are engineered to maintain strong adhesion while being used; but they can be selectively deactivated under external triggers, allowing controlled disassembly.[17,18] Reported on-demand delamination strategies are most commonly based on thermal activation/deactivation, changes in bonding configuration with variations in pH, enzymatic degradation of polysaccharide- or peptide-based glues, light-induced debonding via photoreactive moieties and chemically driven interfacial separation.[17,19] Such designs can be applied in various fields, including wood, electronics and metal bonding.[20,21] However, many debondable adhesive concepts rely on solvent-driven dissolution, harsh chemical triggers or high-energy inputs, which can introduce safety concerns, additional process burdens and potential substrate damage.[22] Besides, no trigger-responsive adhesive has been reported yet for pharmaceutical blister packaging, although strong bonding between plastic and aluminum layers remains an obstacle to recycling. This gap demonstrates the potential benefits of the development of stimuli-responsive glues specifically tailored for blister pack applications.

While designing a stimuli-responsive adhesive, certain natural polysaccharides can be considered as the “glue matrix”, since they may provide additional characteristics such as biodegradability and antimicrobial activity.[23] Proteins, regarded as biodegradable polyamides, can also be used for this purpose, as they readily bind to polymeric surfaces from aqueous solutions at ambient temperature, often achieving surface coverages higher than 80% on synthetic polymers and metals.[24] The later are often referred to as adhesion promoting peptides or “anchor peptides” and can decorate surfaces with hydrophilic and hydrophobic functional groups.[24,25] In detail, anchor peptides (APs), which are short peptides with 20-100 amino acids, provide selective and stable binding, making them valuable tools for surface functionalization.[26] Furthermore, directed evolution strategies such as KnowVolution (Knowledge-Gaining Directed Evolution) enable the tailoring of binding strength,[27] the enhancement of material-binding specificity,[24] the improvement of protein resistance to temperature, pH and ionic liquids and the increase in activity.[28-32] Several studies have demonstrated that engineered-APs can be immobilized on a variety of material surfaces including polymers (e.g. PET, PS, PP) and metals (e.g. stainless steel, gold), as well as fused to enzymes and fluorescent proteins for functional applications.[32-34] In particular, engineered binding peptides and protein domains can be tailored to achieve selective and strong interfacial interactions, enabling surface functionalization across a range of materials. These systems

View Article Online
DOI: 10.1039/D6GC00733C

can also be designed as fusion proteins, combining multiple binding functionalities within a single construct, thereby offering enhanced control over interfacial adhesion.

Here, we propose switchable adhesion as a green processing tool for multilayer blister packaging by combining (i) a renewable polysaccharide matrix (CNC/chitosan), (ii) a genetically engineered bifunctional fusion protein (CBM3-Snakin-1, where CBM3 denotes carbohydrate-binding module 3) for interfacial anchoring and (iii) mild, aqueous triggers (pH shift with mild acid or cellulase treatment) to enable controlled delamination and cleaner separation of aluminum and PVC-based layers. Earlier studies have reported the use of chitosan-protein, cellulose-protein and chitosan/cellulose-based materials for various applications, including bio-inspired adhesive systems.[35-41]. However, these approaches have primarily focused on adhesion performance and generally do not involve engineered fusion proteins for selective interfacial anchoring and controlled debonding, and limited information is available regarding the adhesive or selective delamination behavior of CNC/chitosan/protein-based systems.[42]. After identification of Snakin-1 as an efficient and strong binder to both hard and soft aluminum foils, as well as PVC and PVC-based commercial product, and confirming that CBM3 also binds to CNC and CH as expected; experiments were conducted to determine a suitable glue matrix incorporating the bifunctional fusion protein CBM3-Snakin-1. The resulting system provided a sustainable glue for the recycling of pharmaceutical blister packages by enabling the efficient separation of aluminum foil and PVC-based plastic sheet. Characterization studies revealed enhanced hydrogen bonding interactions in CNC/CH blends. Thermal analyses showed that CNC improved the thermal stability of the CH matrix, while CBM3-Snakin-1 incorporation reduced polymer chain mobility without negatively affecting thermal stability. Debonding tests under temperature, pH and enzymatic stimuli revealed rapid adhesion failure in response to pH and enzymatic triggers, whereas samples exposed to thermal stimuli (in both aqueous and air media) showed slower or no separation. Besides its highly specific debonding behavior, the adhesive's water and temperature resistance also demonstrated its strong potential for commercial use. To assess the potential green advance of the proposed system, the approach was benchmarked against representative debonding-on-demand adhesive strategies using selected green processing metrics. To the best of our knowledge, this approach uniquely integrates a CNC/chitosan matrix with a bifunctional fusion protein to achieve both interfacial anchoring and on-demand debonding.

View Article Online
DOI: 10.1039/D6GC00733C

2. Experimental Methods

2.1. Production of EGFP-Snakin-1 and CBM3-Snakin-1 fusion proteins

Snakin-1, one of the most cysteine-rich peptides, was selected as the anchor peptide for the bio-based glue design due to the affinity of thiol groups in cysteine residues for the chlorine present in PVC.[43] To investigate the binding behavior of Snakin-1 toward the target surfaces, it was cloned into the pET28(+) backbone vector by GenSkript Biotech (Netherlands). Following amplification and design of the synthetic genes, the His_6_eGFP_17xHelix_TEV_AP sequence was obtained.

Surface coating experiments were carried out with EGFP-tethered Snakin-1. Both the EGFP-Snakin-1 fusion protein and negative control EGFP construct were expressed in *Escherichia coli* BL21 (DE3) gold cells. For protein expression, pre-cultures were prepared by incubating the cells overnight in 5 mL of LB media (5 g/L yeast extract, 10 g/L tryptone, 10 g/L NaCl) including 0.1 mM kanamycin (at 37°C, 250 rpm, 70% humidity) (The Sartorius Certomat RM, Germany). Main cultures were inoculated with the precultures in 50 mL of TB media (24 g/L yeast extract, 12 g/L peptone, 4 mL/L glycerol, 2.31 g/L KH_2PO_4, 12.54 g/L K_2HPO_4) including 0.1 mM kanamycin. Incubation at 37°C, 250 rpm, 70% humidity was carried out until the culture reached an optical density (OD_{600nm}) of 0.5-0.6 (Multitron Pro, Infors AG, Switzerland). Isopropyl b-D-1-thiogalactopyranoside (IPTG) was added to the media at a final concentration of 0.1 mM to prevent protein over-expression and the cultures were incubated at 20°C for 24 h. Cells were harvested by centrifugation at 3200 g and 4°C for 15 min (Eppendorf Centrifuge 5810 R, Eppendorf AG, Germany) and the resulting cell pellets were stored at -20°C. The cells were suspended in lysis buffer (5 mLTris-HCl buffer (pH 8.0, 50 mM) per gram of cells supplemented with 1 mg/mL lysozyme 10 µg/mL DNAse) and agitated with a rotary shaker at 40 rpm for 30 min. Cell disruption was then performed by sonicating the suspensions in ice for 5 min (with 15 sec intervals, 70% amplitude) (Sonics Vibra-Cell). The lysates, including soluble proteins, were obtained after centrifugation at 3200 g and 4°C for 60 min (Eppendorf Centrifuge 5810 R, Germany).

The improved adhesive designs were based on incorporating CBM3-Snakin-1 fusion construct into the polysaccharide glue matrices to enable more efficient interactions, particularly with cellulose. For this purpose, CBM3-Snakin1_pET-28(+) gene was obtained from GenScript company and transformed into chemically competent *E. coli* BL21 (DE3) cells. Protein expression was then performed as described above.

2.2. Purification of the fusion proteins

View Article Online
DOI: 10.1039/D6GC00733C

The expressed proteins were purified via liquid chromatography technique. Protino Ni-IDA Packed Columns were used for the purification of the His-tagged constructs. Purification efficiency was evaluated by sodium dodecyl sulfate polyacrylamide gel electrophoresis (SDS-PAGE) using a 5% stacking gel and a 12% separating gel. After DNA isolation using NucleoSpin DNA purification kit, sequence analysis was carried out by Eurofins Genomics (see Supplementary Information). The purified proteins were subsequently buffer-exchanged into Tris-HCl (pH 8.0, 50 mM) and concentrated using Amicon protein concentrators before being stored for further applications.

2.3. Assessment of EGFP-Snakin-1 to the plastic and aluminum foil surfaces

PVC (GoodFellow, CAS No: 9002-86-2, Thickness: 0.2 mm), commercial pharmaceutical blister package (PERLALUX® - Duplex, Perlen Packaging, Germany) and aluminum foil (commercial hard and soft foil) sheets were cut into 0.5 cm x 0.5 cm pieces and treated with N_2 to remove the impurities before the surface binding experiments. A 20 µL of EGFP-Snakin-1 solution (with a concentration of 20 µM) was dropped onto the surfaces and kept in dark for 1 h. The dull side of the aluminum foil was selected, since it corresponds to the surface bonded to plastics in the blister package structures. After incubation, the samples were washed thoroughly with Tris-HCl buffer (pH 8.0, 50 mM) to prevent the nonspecific EGFP adsorption in the absence of AP. Fluorescence microscopy analyses were then carried out using confocal microscope (Olympus BX51, Japan).

2.4. Glue design

For the glue design, adhesion performances of 20% (w/v) cellulose nanocrystals (CNC, Nanografi) suspension in DI water, as well as 2% and 5% (w/v) of low molecular weight chitosan (CH, Sigma Aldrich, CAS No: 9012-76-4) solution in 10% (v/v) acetic acid solution were investigated individually and together at CNC to CH mass ratios of 1.0 (CNC/CH) and 0.5 (CNC/2CH). AP effect on the adhesion performance of the polysaccharides was examined by adding 1.8 µM of CBM3-Snakin-1 solution to the surfaces. The adhesive formulations investigated in this study are summarized in Table 1.

View Article Online
DOI: 10.1039/D6GC00733C

Table 1. Overview of adhesive formulations investigated in this study, including composition and presence of CBM3-Snakin-1

ID	Formulation	CNC (% w/v)	CH (% w/v)	CBM3-Snakin-1	CNC:CH mass ratio
1	CNC	20	-	-	-
2	CNC/CBM3-Snakin-1	20	-	✓	-
3	CH (2%)	-	2	-	-
4	CH (2%)/CBM3-Snakin-1	-	2	✓	-
5	CH (5%)	-	5	-	-
6	CH (5%)/CBM3-Snakin-1	-	5	✓	-
7	CNC/CH (2%)	20	2	-	1:1
8	CNC/CH (2%)/CBM3-Snakin-1	20	2	✓	1:1
9	CNC/2CH (2%)	20	2	-	1:2
10	CNC/2CH (2%)/CBM3-Snakin-1	20	2	✓	1:2
11	CNC/CH (5%)	20	5	-	1:1
12	CNC/CH (5%)/CBM3-Snakin-1	20	5	✓	1:1
13	CNC/2CH (5%)	20	5	-	1:2
14	CNC/2CH (5%)/CBM3-Snakin-1	20	5	✓	1:2

2.5. Adhesion of the surfaces

The commercial plastic material and aluminum foil sheets were cut and prepared according to the ASTM F-88 Standard (Standard Test Method for Seal Strength of Flexible Barrier Materials). After cleaning the surfaces, CBM3-Snakin-1 solutions and adhesives were spread on the surfaces homogeneously. The plastic and aluminum surfaces were combined and pressed using clamps that covered the entire glued area and then kept at room temperature for 4 days.

2.6. Characterization studies

The peel tests were performed by using a tensile tester (Zwick Roell Z005, Germany) according to the ASTM F-88 Standard. Free tail method was preferred with a constant jaw moving rate of 11 in/min[44]. Average strength values were indicated after six measurements. Fourier transform infrared spectroscopy (FTIR) analysis was performed with a PerkinElmer Spectrum 3 spectrometer, operating at a resolution of 4 cm^{-1}, and measurements were taken

View Article Online
DOI: 10.1039/D6GC00733C

over a wavenumber range of 4000-400 cm^{-1}. X-ray photoelectron spectroscopy (XPS) analyses were performed to determine the surface elemental composition and chemical states of the samples (Kratos Analytical AXIS Supra +). The thermal properties were analyzed by using a simultaneous thermal analyzer (Perkin Elmer STA 6000). The samples were heated in the range of 35-500°C at a heating rate of 10°C/min under nitrogen atmosphere. Differential scanning calorimetry (DSC) analyzes of the samples were performed from 40°C to 300°C at a heating rate of 10°C/min (Perkin Elmer DSC 8500).

2.7. Debonding studies

The debonding patterns of the glued surfaces with CH (5%), CH (5%)/CBM3-Snakin-1, CNC/CBM3-Snakin-1, CNC/CH (5%)/CBM3-Snakin-1 were investigated under the effects of temperature, pH and enzyme (cellulase from *Trichoderma reesei*, aqueous solution, ≥700 units/g (Sigma, CAS No: 9012-54-8)) triggers. The conditions of these experiments were listed in Table 2.

Table 2. The conditions at which debonding patterns of the glued surfaces investigated

No	Trigger	Ambient media	Temperature	Agitation rate
1	-	Distilled water	30°C	750 rpm
2	Temperature	Distilled water	95°C	750 rpm
3	Temperature	Air	95°C	-
4	pH	10% (v/v) acetic acid solution	30°C	750 rpm
5	Enzyme (cellulase)	Aqueous solution	60°C	750 rpm

3. Results and Discussion

3.1. Visualization of EGFP-Snakin-1 binding on the target surfaces

The binding behavior of EGFP and EGFP-Snakin-1 constructs on aluminum foil, PVC and commercial packaging material was investigated and the corresponding fluorescence microscope images were presented in Figure 1. None of the surfaces showed auto-fluorescence and no significant fluorescence signals were detected for the EGFP protein (without AP) in any of the cases studied. EGFP-Snakin-1 was found to bind to all of the surfaces examined, demonstrating that Snakin-1 is an excellent primer for PVC and aluminum sheets.

View Article Online
DOI: 10.1039/D6GC00733C

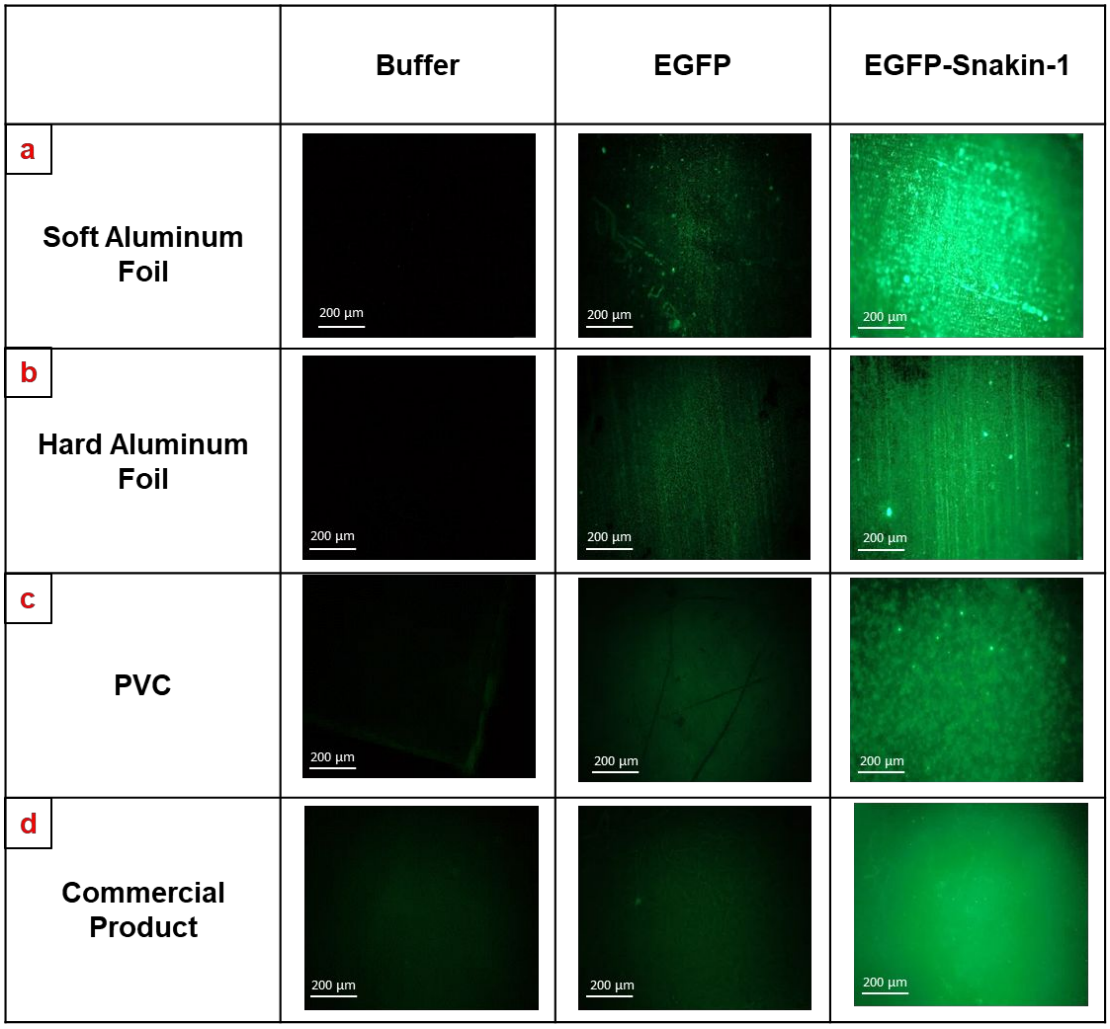

Figure 1. Fluorescence images of (a) soft aluminum foil, (b) hard aluminum foil, (c) PVC and (d) commercial plastic sheets, which were incubated in 50 mM Tris/HCl pH 8.0, 20 μM EGFP solution and 20 μM EGFP-Snakin-1 solution

3.2. Glue design

3.2.1. Adhesion performance of neat CNC and CH systems with and without CBM3-Snakin-1

CNC was preferred considering its very high mechanical strength and modifiable chemical structure.[45] Although it provided some adhesive effect, the resulting dry bond strength and the essential physicochemical properties required for commercial applications needed improvement. Therefore, chitosan (CH) was incorporated as a dispersing agent, since it contains both hydroxyl and amino groups enabling various intermolecular interactions.[46] Moreover, its tendency to bind to low-surface-energy materials (such as plastics) and its favorable physical properties (i.e., increased hydrophobicity, smoothness and viscosity, allowing for easy surface dispersion) make it highly advantageous.[47]

View Article Online
DOI: 10.1039/D6GC00733C

Before developing the improved glue formulation, the effects of CBM3-Snakin-1 on the binding behavior of individual CNC and CH were examined. The binding strength of the 5% (w/v) CH solution was more than 2.5 and 3.5 times higher than those of the 2% (w/v) CH solution and 20% (w/v) CNC suspension, respectively, and the addition of CBM3-Snakin-1 consistently resulted in a trend toward increased adhesion across all these formulations (Figure 2). On the other hand, photographs of the bonded sheets after adhesion failure revealed that CNC alone exhibited a higher affinity for the aluminum foil, whereas the addition of CBM3-Snakin-1 enhanced adhesion toward the plastic surface. As expected, both CH and CH/CBM3-Snakin-1 adhesives were predominantly retained on the plastic substrate after separation (Figure 3).

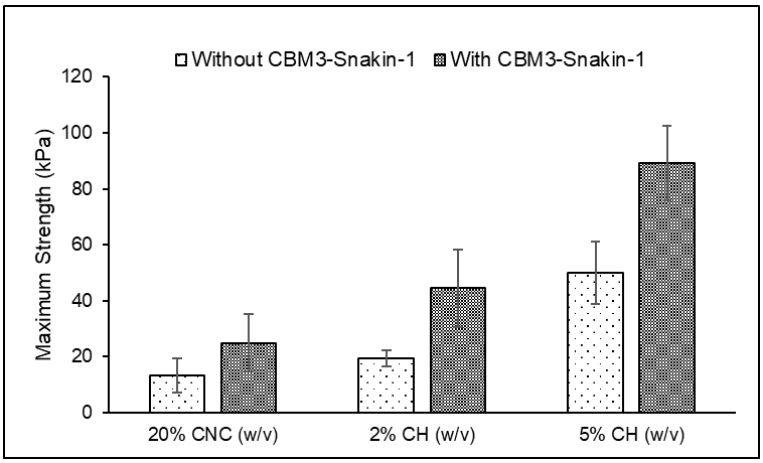

Figure 2. Maximum adhesion strength values for samples prepared using 20% (w/v) CNC and CH solutions at 2% and 5% (w/v), with and without CBM3-Snakin-1.

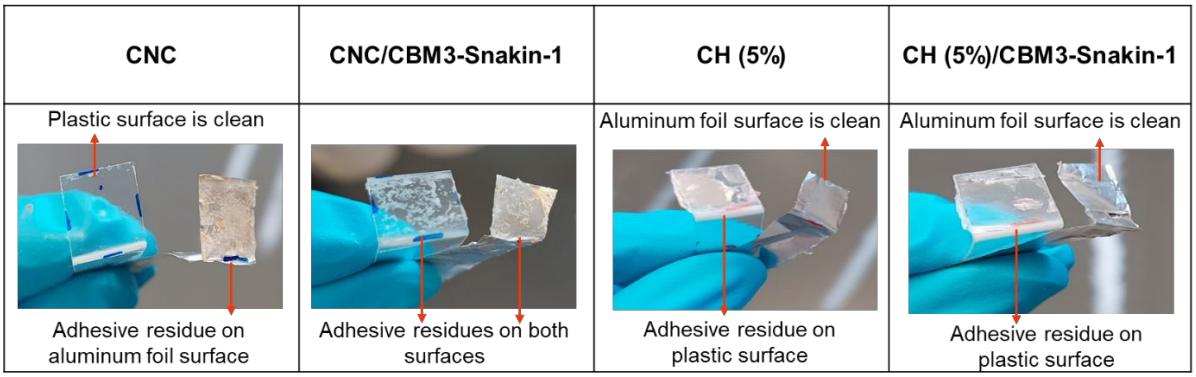

Figure 3. Photographs of fracture surfaces after adhesion failure for different adhesive formulations, showing the distribution of adhesive residues on aluminum and plastic substrates

3.2.2. Adhesion performance of CNC/CH blends with and without CBM3-Snakin-1

Adhesion characteristics of CNC-CH blends were examined by incorporating 20% (w/v) CNC suspension with 5% and 2% (w/v) CH solutions at CNC-to-CH mass ratios of 1.0 (CNC/CH)

View Article Online
DOI: 10.1039/D6GC00733C

and 0.5 (CNC/2CH) (Figure 4). The findings showed that samples including 5% (w/v) CH exhibited improved adhesion in all cases studied. In addition, the incorporation of CBM3-Snakin-1 into the formulation containing equal amounts of CNC and CH doubled the adhesion strength, making CNC/CH (5%)/CBM3-Snakin-1 the most promising formulation in terms of bonding performance; however, no significant improvement was observed for formulations containing 2% (w/v) CH. This behavior is consistent with the idea that the contribution of CBM3-Snakin-1 to adhesion strength is strongly dependent on the properties of the polysaccharide matrix. At lower CH concentration (2% w/v), the CNC/CH system likely forms a less cohesive and less continuous network, limiting efficient stress transfer throughout the adhesive layer. In addition, the lower availability of accessible binding regions for CBM3-Snakin-1 may have resulted in incomplete interfacial coverage, thereby reducing the contribution of protein-mediated anchoring to the overall adhesion strength.[48,49]

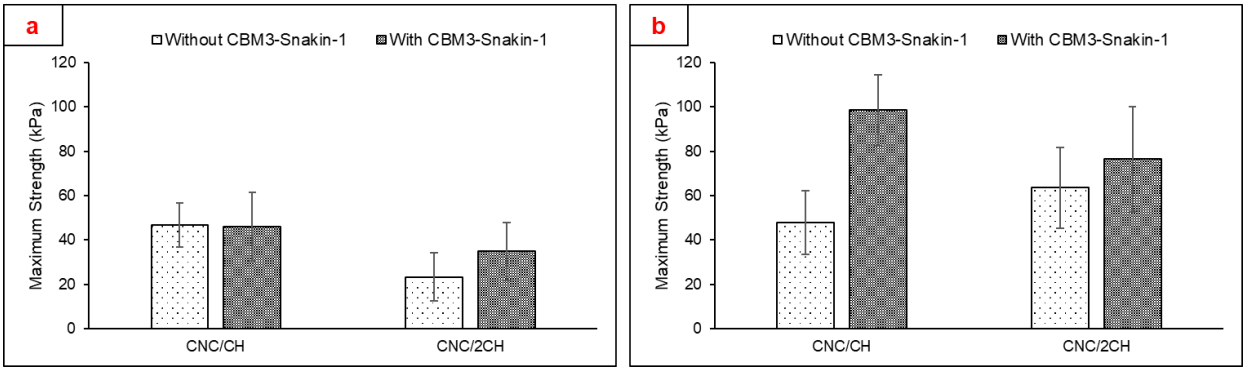

Figure 4. Maximum adhesion strength values obtained from the samples glued with CNC/2CH and CNC/CH adhesives without and with CBM3-Snakin-1: (a) CH concentration is 2% (w/v), (b) CH concentration is 5% (w/v)

3.3. Characterization studies

3.3.1. FTIR

Infrared spectra of the CH (5%), CNC, CNC/2CH (5%) and CNC/CH (5%) samples were shown in Figure 5. In the spectrum of CH, the broad peak at 3316 cm^{-1} corresponded to combination of O-H and N-H stretching vibrations. The peaks at 2922 and 2855 cm^{-1} belonged to the symmetric and asymmetric C-H vibrations, respectively.[50] The absorption bands at 1657 and 1545 cm^{-1} were ascribed to presence of C=O stretching and N-H bending of amide I and amide II, respectively. [51] The peak observed at 1151 cm^{-1} showed the existence of asymmetric C-O-C stretching of the glucose ring.[52,53] While the peaks seen at 1064 and 1019 cm^{-1} were attributed to C-O stretching, the band at 897 cm^{-1} demonstrated the presence of the pyranose ring. For the CNC sample, the broad band centered at around 3312 cm^{-1} was assigned to the

View Article Online
DOI: 10.1039/D6GC00733C

stretching vibrations of O-H groups, revealing the extensive hydrogen bonding network within the cellulose structure. The symmetric bending of CH_2 was verified with the peak observed at 1437 cm^{-1}, which are commonly associated with the crystalline regions of cellulose. The peak at 1308 cm^{-1} corresponded to the C-H and C-O bending vibrations.[54] The peak at 1037 cm^{-1} was attributed to the C-O-C stretching of the D-glucose units existing in cellulose I and cellulose II.[55] When CNC and CH were blended, the peak observed at around 3300 cm^{-1} became broader, which is consistent with an increased distribution of hydrogen-bonded O-H and/or N-H groups. In addition, hydrogen-bonding interactions also contributed to the reduced resolution and increased overlap of the C-H stretching bands around 2922 and 2855 cm^{-1} observed in neat CH.[56] Changes in the amide/amine-related region (at around 1545 cm^{-1}) further indicated the altered chemical environment of CH functional groups, consistent with enhanced intermolecular interactions in the CNC/CH network[57] (Figure 5a and 5d). A simplified schematic illustration of the proposed intermolecular hydrogen-bonding interactions between CH and CNC is presented in Figure 6.

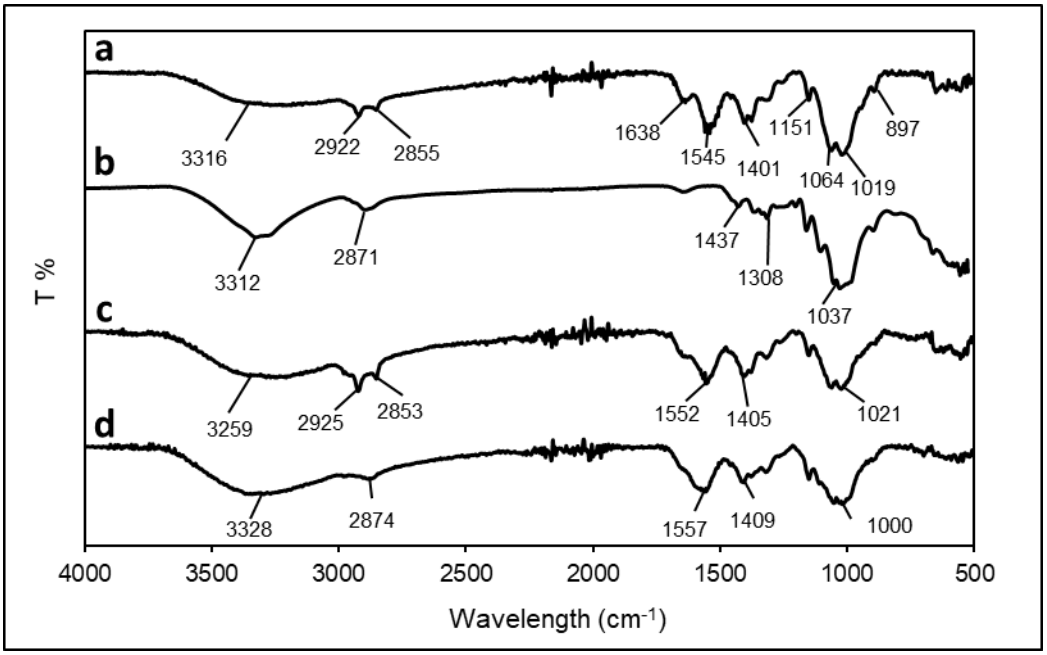

Figure 5. FTIR spectra of (a) CH (5%), (b) CNC, (c) CNC/2CH (5%), (d) CNC/CH (5%)

View Article Online
DOI: 10.1039/D6GC00733C

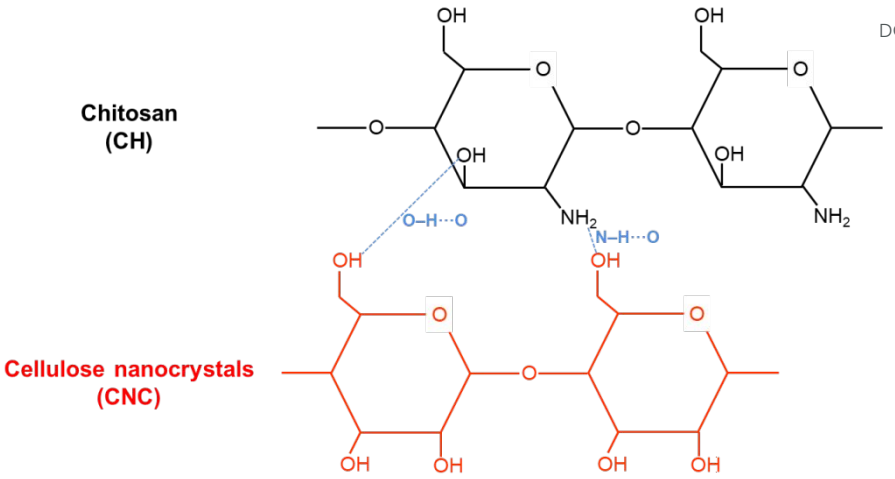

Figure 6. Proposed intermolecular hydrogen-bonding interactions between CH and CNC within the blended network

3.3.2. XPS:

The surface chemistry of CNC/CH (5%) and CNC/CH (5%)/Snakin-1 samples were investigated via XPS analyzes (Figure 6). The broad peak at 399.4 eV and the small peak at 400.6 eV arose from the neutral and protonated amines, respectively, due to the presence of CH (Figure 7b-i). CBM3-Snakin-1 addition resulted in significant increase in the intensities of both peaks, as expected (Figure 7b-ii). Three peaks existing at 284.9, 286.1 and 287.7 eV attributed to the carbon (C_{1s}) atoms in C-C/C-H, C-O/C-N and O-C-O bonds, respectively (Figure 7a-i).[58-60] The intensities of the peaks observed at around 284 and 287 eV increased due to the increase in aliphatic carbon atoms and amide linkages after CBM3-Snakin-1 addition; while it led to a decrease in the intensity of the peak at 286 eV, as the peptide was not rich in C-O linkages compared to polysaccharides (Figure 7a-ii).[61] The O_{1s} spectra; which indicated the increase and decrease in the intensities of the peaks at 530.9 eV (associated with C=O bonds) and 532.7 eV (associated with C-O bonds), respectively, were also found to be consistent with the C_{1s} results (Figure 7c-i and ii).

View Article Online
DOI: 10.1039/D6GC00733C

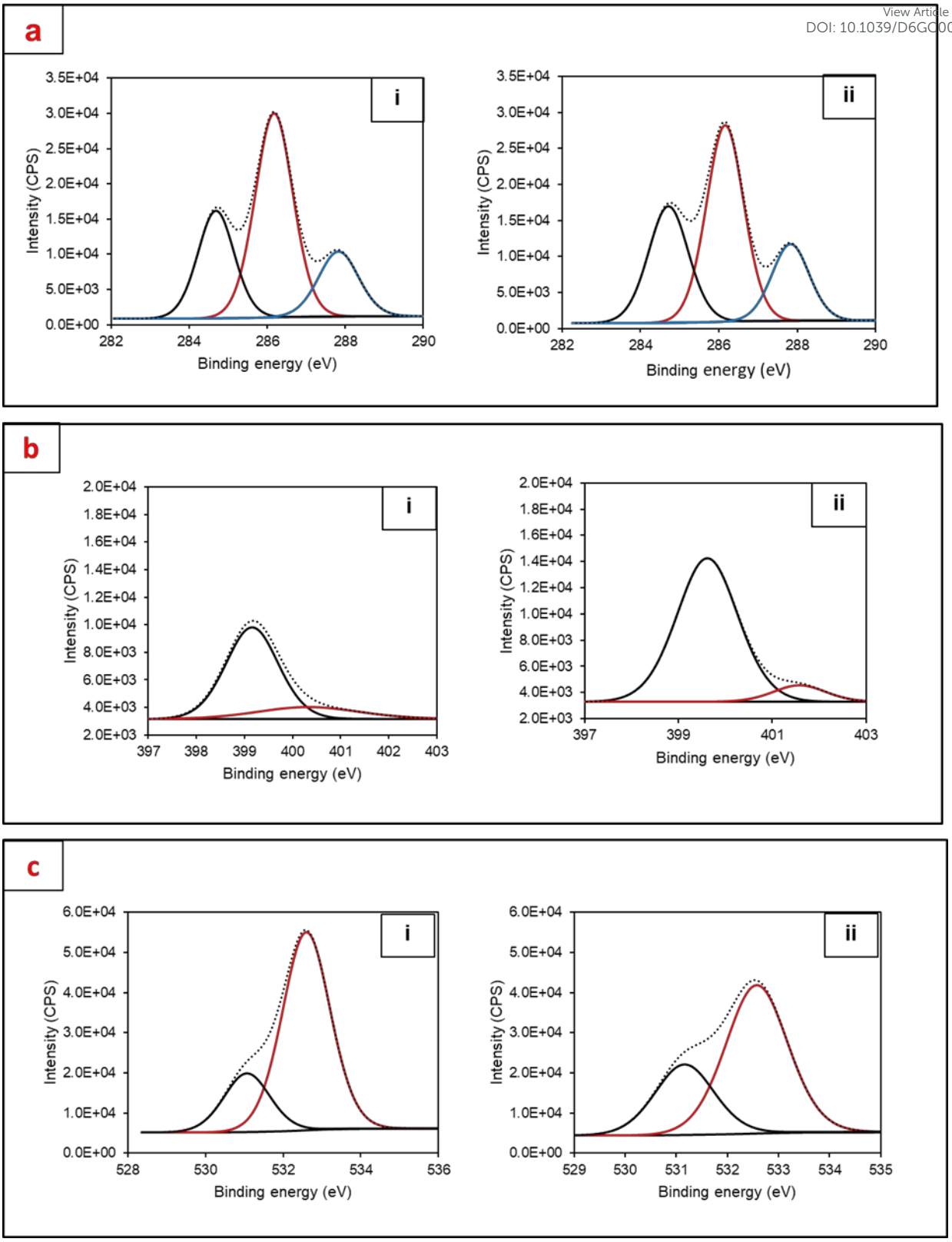

Figure 7. XPS spectra of (i) CNC/CH (5%) and (ii) CNC/CH (5%)/CBM3-Snakin-1; a) C_{1s} scans, b) N_{1s} scans, c) O_{1s} scans

3.3.3. TGA:

View Article Online
DOI: 10.1039/D6GC00733C

TGA analyses were carried out to evaluate the effect of CNC incorporation on the thermal degradation characteristics of CH (Figure 8a). TGA curves of both neat CH and CNC/CH (5%) composite samples exhibited a three-stage degradation processes. In the first stage, a minor weight reduction occurred at around 100°C corresponding to the evaporation of physically absorbed water molecules. The second stage, occurring between approximately 150-380°C, represented the major decomposition of the constituents, primarily associated with the breakdown of glycosidic bonds in CNC and CH. Notably, the T_{onset} value of neat CH was around 200°C, whereas the addition of CNC increased this value to approximately 230°C, indicating the significant enhancement in the resistance of the material to thermal decomposition.[62] The additional incorporation of CBM3-Snakin-1 fusion protein did not compromise this stability. At higher temperatures, the third stage was observed, during which pyrolysis of the polysaccharides led to the formation of char-like residuals.

3.3.4. *DSC:*

DSC analyses were performed to investigate the thermal behaviors of CH (5%), CNC/CH (5%) and CNC/CH (5%)/CBM3-Snakin-1 samples and the results were shown in Figure 8b. The thermogram of CH was consistent with previously reported data. The endothermic peak at around 100°C corresponded to the loss of absorbed water and the exothermic peak at approximately 276°C was related to the decomposition of amine (GlcN) units.[63,64] After the incorporation of CNC into CH, the exothermic peak became broader, indicating that the thermal transition processes occurred over a wider temperature range. This change may be attributed to the hydrogen bond formation between CH and CNC and/or improved heat transfer pathways generated by well-dispersed CNC within CH matrix.[65] Interestingly, the addition of CBM3-Snakin-1 to the CNC/CH sample resulted in complete disappearence of this peak, due to the strong hydrogen bonds formed between CBM3 and the polysaccharides, which can restrict polymer chain mobility and contribute to enhance the thermal stability of the resulting composite.[66]

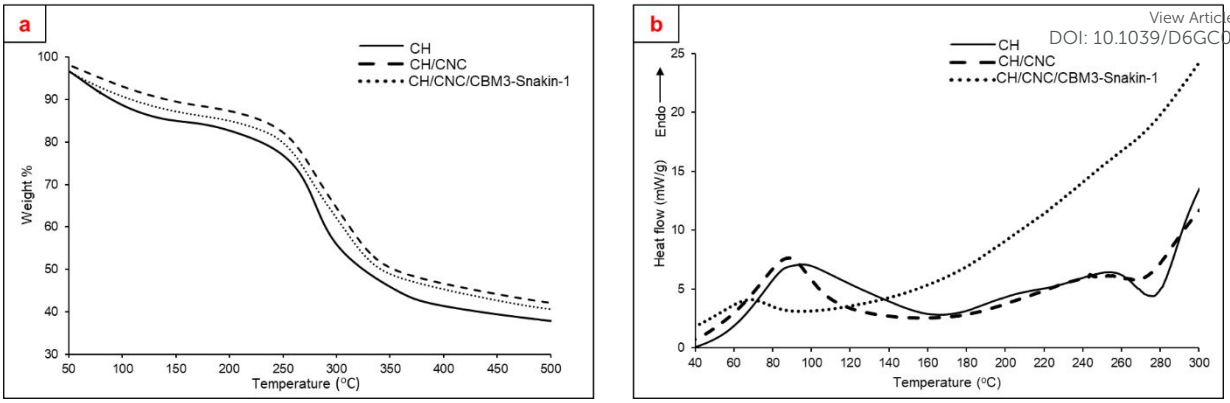

Figure 8. (a) TGA and (b) DSC curves of CNC, CNC/CH (5%) and CNC/CH (5%)/CBM3-Snakin-1 samples

3.4. Debonding Studies

A stimuli-responsive adhesive design must be both time- and cost-efficient to be suitable for large-scale applications. Another crucial aspect is ensuring that each surface can be retrieved intact, without any damage such as decomposition, melting, or corrosion.[19,67] Within this scope, the effects of temperature (in both aqueous and air environments) and pH were examined, in addition to experiments investigating the influence of using the cellulase enzyme as a trigger (Table 3). In aqueous media, no separation occurred at 30°C, whereas samples glued with CH (5%) and CNC/CH (5%)/CBM3-Snakin-1 debonded at 95°C within 35-40 min, due to changes in chitosan's water-holding capacity and crystallinity affecting hydrogen bonding configurations.[68] On the other hand, no failure was observed in any of the samples that were kept in an oven at 95°C for several days. The most striking result was obtained in the pH-triggering experiments: While the adhesives composed of only CH (5%) or CH (5%)/CBM3-Snakin-1 failed in 10% acetic acid solution after 45-50 min, the surfaces bonded with CNC-containing glues debonded very rapidly, within approximately 5 min. Here, the dissolution of CH, the swelling of CNC and the loss of CBM3 activity in the acidic medium led to the controlled separation while keeping the substrates intact.[69,70] Another characteristic debonding behavior was observed after cellulase treatment. Upon incubation in an aqueous cellulase solution, the samples bonded with CNC/CBM3-Snakin-1 did not separate due to competition between CBM3 and cellulase for CNC binding sites. In contrast, the samples bonded with CNC/CH (5%)/CBM3-Snakin-1 adhesives debonded within 15 min. This clear distinction demonstrates the crucial role of CH to enhance enzyme-triggered debonding by designing polysaccharide network that is more accessible and also responsive to enzymatic activity. The observed debonding within approximately 15 min demonstrates the potential for relatively rapid separation under mild conditions; however, "acceptable processing times" in industrial recycling are process-dependent and may vary depending on system design and scale.

View Article Online
DOI: 10.1039/D6GC00733C

Nevertheless, the debonding achieved in this study occurs within timeframes comparable to typical washing or treatment steps used in polymer recycling processes, supporting its practical relevance.[71,72]. In the blister-pack recycling literature, separation processes are generally evaluated in terms of separation efficiency rather than explicitly defined industrial processing times. However, available studies indicate that blister-pack layer separation processes can span a wide range of timescales, from minutes to several days depending on the process conditions.[73-75]. Accordingly, the ~15 min debonding time achieved in the present study appears feasible within the context of reported blister-pack separation approaches.

The results collectively demonstrated the water and temperature resistance of the designed adhesives, as well as their characteristic debonding behaviors under different external triggers. Among these findings, acetic acid treatment was identified as the most promising trigger, as it enabled a highly selective stimuli-responsive debonding process for the samples bonded with the CNC/CH (5%)/CBM3-Snakin-1 adhesive, which was also confirmed to be the strongest formulation. Such a rapid and low-cost stimuli-responsive separation process, with the adhesive being readily removable from the surface, appears highly advantageous for large-scale applications. Moreover, these samples were the only ones that responded to the cellulase treatment, making this study a pioneering contribution in the field. While cellulase was selected in this study due to its specificity toward the cellulose-based matrix, the use of proteases or enzyme combinations could offer additional control over debonding kinetics by modulating interfacial protein cleavage, representing an interesting direction for future work.

Table 3. Debonding behavior of the adhered surfaces under different conditions

Required Time for Separation (min)				
Ambient Media	**CH (5%)**	**CH (5%)/CBM3-Snakin-1**	**CNC/CBM3-Snakin-1**	**CNC/CH (5%)/CBM3-Snakin-1**
Distilled water at 30°C	Not separated	Not separated	Not separated	Not separated
Distilled water at 95°C	40±8	Not separated	Not separated	35±6
Air at 95°C	Not separated	Not separated	Not separated	Not separated
10% (v/v) acetic acid solution at 30°C	50±5	45±5	5±2	2±1
Cellulase solution at 60°C	Not separated	Not separated	Not separated	15±4

View Article Online
DOI: 10.1039/D6GC00733C

3.5. Green advance assessment through benchmarking of debonding-on-demand adhesive strategies

To provide clear evidence of the green advance of the proposed bonding-debonding concept, the present approach was benchmarked against representative debonding-on-demand adhesive strategies reported in the literature, including solvent-driven systems, thermally triggered release, photo- or electro-triggered systems and dynamic covalent adhesives.[76] Following the "Measuring Green Chemistry" guidance,[77] the green advance is qualitatively assessed using clearly-defined criteria (i.e. hazardous auxiliaries, energy input for debonding, process complexity and end-of-life separation quality), as summarized in Table 4. Overall, the proposed system offers several advantages from a green processing perspective. In contrast to approaches requiring organic solvents, high-energy activation or specialized equipment; the present system operates under aqueous conditions and enables debonding either by a mild pH shift (acetic acid-based trigger) or by cellulase treatment, both of which are compatible with scalable and lower-hazard processing. Combined with the use of renewable polysaccharide components and the ability to achieve selective delamination of multilayer blister substrates, this approach represents a promising strategy for enabling more sustainable adhesive systems and facilitating end-of-life material separation.

Table 4. Comparison of representative debonding-on-demand adhesive strategies based on selected green processing metrics, including trigger mechanism, auxiliary chemical requirements, energy input and implications for end-of-life material separation.

Approach (representative)	Primary trigger	Hazardous auxiliaries	Energy input for debonding	Process complexity	End-of-life separation quality	References
Solvent-driven debonding/swelling	Solvent	Organic solvent or solvent mixtures often required.	Low/moderate; but solvent recovery may be needed	Solvent handling and removal steps	Separation possible; but contamination or residue risk	22, 78
Thermal debonding adhesives	Heat	Usually none; but additives possible	High energy input due to elevated temperatures	Heating equipment required	Separation possible; but substrate damage risk	79, 80
Photo- or electro-triggered systems	UV/light/electric	Photoinitiators or conductive fillers may be required	Moderate energy input (irradiation/electric stimulus)	Specialized irradiation equipment may be required; limited light penetration in opaque multilayer substrates	Separation possible	19, 22
Dynamic covalent bonded reversible adhesives	Chemical stimulus	Chemical triggers, catalysts or reagents often required	Moderate; depends on trigger chemistry	Trigger chemistry may be complex	Network disassembly possible	81-83
This work (CNC/CH/ CBM3-Snakin-1)	Mild pH shift OR cellulase	None; aqueous trigger media	Low-to-moderate; ambient acidic treatment OR enzymatic treatment at 60°C	Simple aqueous treatment	Clean delamination of Al/PVC-based layers	–

View Article Online
DOI: 10.1039/D6GC00733C

Conclusion

Here, a fully biobased glue composed of a CNC/CH biocomposite incorporating the bifunctional fusion peptide CBM3-Snakin-1 was developed, introducing a bio-based adhesive concept that combines pH- and enzyme (cellulase)-triggered debonding. Switchable bonding and debonding on the demand represents a key technology for the circular economy with a proof of concept demonstrated on blister packages composed of PVC-based plastic and aluminum layers. After establishing Snakin-1 as a strong binder to plastic and aluminum surfaces and confirming CBM3's affinity toward CNC and CH, a bifunctional CBM3-Snakin-1 fusion protein was incorporated into a bio-based adhesive matrix to optimize bonding performance. The developed adhesive exhibited high bonding strength, selective pH- and enzyme-triggered debonding and strong resistance to water and temperature, confirming its high feasibility for practical blister packaging applications. The glue can be applied using scalable coating methods such as dip coating or spraying. By exchanging Snakin-1, it can be tailored for various synthetic and natural polymers, metals/alloys, ceramics or natural surfaces, suggesting broad applicability of the switchable adhesive systems for the composite materials.

Author contributions

Hande Günan: Investigation, Methodology, Validation, Visualization, Writing - Original Draft
Mariia Vorobii: Methodology, Supervision
Ulrich Schwaneberg: Conceptualization, Supervision, Resources, Writing - Review & Editing

Data availability

The data supporting the findings of this study are available within the article and its Electronic Supplementary Information (ESI).

Acknowledgement

This research was funded by German Federal Ministry of Education and Research (BMFTR) (grant number: 031B1148A). We also acknowledge the financial support awarded to H. Günan by the Scientific and Technological Research Council of Türkiye (TÜBİTAK) under BİDEB-2219 International Postdoctoral Research Fellowship Program (grant number: 1059B192203099) and we thank Perlen Packaging (Germany) for providing the products used in this study.

View Article Online
DOI: 10.1039/D6GC00733C

References:

1. M. Mandal, A. Roy, R. Popek and A. Sarkar, Micro- and nano- plastic degradation by bacterial enzymes: A solution to 'White Pollution', *Microbe*, 2024, **3**, 100072.

2. S. Allen, D. Allen, S. Karbalaei, V. Maselli and T. R. Walker, Micro(nano)plastics sources, fate, and effects: What we know after ten years of research, *J. Hazard. Mater. Adv.*, 2022, **6**, 100057.

3. M. S. Yee, L. W. Hii, C. K. Looi, W. M. Lim, S. F. Wong, Y. Y. Kok, B. K. Tan, C. Y. Wong and C. O. Leong, Impact of microplastics and nanoplastics on human health, *Nanomaterials (Basel)*, 2021, **11**, 2.

4. B. H. Dastjerdi, V. Strezov, R. Kumar and M. Behnia, Economic Feasibility and sustainability assessment of residual municipal solid waste management scenarios in NSW, Australia, *Sustainability*, 2021, **13**, 16.

5. Y. Yang, R. Boom, B. Irion, D.-J. van Heerden, P. Kuiper and H. de Wit, Recycling of composite materials, *hem. Eng. Process.: Process Intensif.*, 2012, **51**, 53-68.

6. İ. Yaren Çapkın and M. Gökelma, A review on characterization and recyclability of pharmaceutical blisters, *Cleaner Waste Syst.*, 2023, **4**, 100082.

7. S. Shukla, P. Halli, M. K. Khalid and M. Lundström, Waste pharmaceutical blister packages as a source of secondary aluminum, *JOM*, 2022, **74**, 2, 612-621.

8. Y. Shin, Y. Qiao, Y. Ni, J. L. Ramos, E. K. Nickerson, D. R. Merkel and K. L. Simmons, Interfacial bond characterization of epoxy adhesives to aluminum alloy and carbon fiber-reinforced polyamide by vibrational spectroscopy, *Surf. Interfaces*, 2023, **42**, 103346.

9. A. C. Marques, A. Mocanu, N. Z. Tomić, S. Balos, E. Stammen, A. Lundevall, S. T. Abrahami, R. Günther, J. M. M. de Kok and S. Teixeira de Freitas, Review on adhesives and surface treatments for structural applications: Recent developments on sustainability and implementation for metal and composite substrates, *Materials (Basel)*, 2020, **13**, 24.

10. K. Kremser, H. Schön, P. Gerl, M. Á. V. Gómez, D. R. Espinosa, A. Morandini, M. P. Argilés, B. M. Martínez and G. M. Guebitz, Pharmaceutical blister waste recycling using biogenic sulfuric acid: Effect of sulfur source and blister material on bioleaching efficiency, *Hydrometallurgy*, 2023, **221**, 106124.

11. S. Al-Alimi, N. K. Yusuf, A. M. Ghaleb, M. A. Lajis, S. Shamsudin, W. Zhou, Y. M. Altharan, H. S. Abdulwahab, Y. Saif, D. H. Didane, I. S T T and A. Adam, Recycling aluminium for sustainable development: A review of different processing technologies in green manufacturing, *Results Eng.*, 2024, **23**, 102566.

12. S. Gudić, L. Vrsalović, J. Krolo, A. Nagode, I. Dumanić Labetić and B. Lela, Corrosion behaviour of recycled aluminium AlSi9Cu3(Fe) machining chips by hot extrusion and thixoforming, *Sustainability*, 2024, **16**, 4.

13. C. Gnoffo, R. Arrigo and A. Frache, Mechanical recycling of HDPE-based packaging: Interplay between cross contamination, aging and reprocessing, *Polym. Degrad. Stab.*, 2025, **236**, 111290.

View Article Online
DOI: 10.1039/D6GC00733C

14. A. Chidara, K. Cheng and D. Gallear, Engineering innovations for polyvinyl chloride (PVC) recycling: A systematic review of advances, challenges, and future directions in circular economy integration, *Machines*, 2025, **13**, 5.

15. E. U. Thoden van Velzen, S. Chu, F. Alvarado Chacon, M. T. Brouwer and K. Molenveld, The impact of impurities on the mechanical properties of recycled polyethylene, *Packag. Technol. Sci.*, 2021, **34**, 4, 219-228.

16. E. Bezeraj, S. Debrie, F. J. Arraez, P. Reyes, P. H. M. Van Steenberge, D. R. D'Hooge and M. Edeleva, State-of-the-art of industrial PET mechanical recycling: Technologies, impact of contamination and guidelines for decision-making, *RSC Sustain.*, 2025, **3**, 5, 1996-2047.

17. Z. Liu and F. Yan, Switchable adhesion: On-demand bonding and debonding, *Adv. Sci. (Weinh)*, 2022, **9**, 12, e2200264.

18. J. Lv, D. Zhang, X. Li, Y. Miao, Y. Wang, Y. Wang and X. Zhang, Reversible biobased adhesives enable closed-loop engineered composites, *Nat. Commun.*, 2025, **16**, 1, 7871.

19. N. D. Blelloch, H. J. Yarbrough and K. A. Mirica, Stimuli-responsive temporary adhesives: Enabling debonding on demand through strategic molecular design, *Chem. Sci.*, 2021, **12**, 46, 15183-15205.

20. J. L. Thoma, R. Elsener, I. Burgert and M. Schubert, Chemical and physical debonding-on-demand of poly(urethane urea) thermoset adhesives to facilitate the recycling of engineered wooden products, *ACS Appl. Polym. Mater.*, 2024, **6**, 10, 5778-5787.

21. I. Bibi, H. Ahmad, A. Farid, H. Iqbal, N. Habib and M. Atif, A comprehensive study of electrically switchable adhesives: Bonding and debonding on demand, *Mater. Today Commun.*, 2023, **35**, 106293.

22. C. Bandl, W. Kern and S. Schlögl, Adhesives for “debonding-on-demand”: Triggered release mechanisms and typical applications, *Int. J. Adhes. Adhes.*, 2020, **99**, 102585.

23. A. Ali, K. Rehman, H. Majeed, M. F. Khalid and M. S. H. Akash, in *Green Adhesives*, 2020, DOI: https://doi.org/10.1002/9781119655053.ch8, ch. AMA Arch. Derm., pp. 165-180.

24. M. Mao, L. Ahrens, J. Luka, F. Contreras, T. Kurkina, M. Bienstein, M. Sária Pereira de Passos, G. Schirinzi, D. Mehn, A. Valsesia, C. Desmet, M.-Á. Serra, D. Gilliland and U. Schwaneberg, Material-specific binding peptides empower sustainable innovations in plant health, biocatalysis, medicine and microplastic quantification, *Chem. Soc. Rev.*, 2024, **53**, 12, 6445-6510.

25. J. L. McKenzie, T. J. Webster and J. L. McKenzie, in *Biomedical Materials*, ed. R. Narayan, Springer International Publishing, Cham, 2021, DOI: 10.1007/978-3-030-49206-9_12, pp. 399-422.

26. J. Dittrich, C. Brethauer, L. Goncharenko, J. Bührmann, V. Zeisler-Diehl, S. Pariyar, F. Jakob, T. Kurkina, L. Schreiber, U. Schwaneberg and H. Gohlke, Rational design yields molecular insights on leaf-binding of anchor peptides, *ACS Appl. Mater. Interfaces*, 2022, **14**, 25, 28412-28426.

27. K. Rübsam, M. D. Davari, F. Jakob and U. Schwaneberg, KnowVolution of the polymer-binding peptide LCI for improved polypropylene binding, *Polymers (Basel)*, 2018, **10**, 4.

28. Y. Lu, K.-W. Hintzen, T. Kurkina, Y. Ji and U. Schwaneberg, Directed evolution of material binding peptide for polylactic acid-specific degradation in mixed plastic wastes, *ACS Catal.*, 2023, **13**, 19, 12746-12754.

29. F. Contreras, M. J. Thiele, S. Pramanik, A. M. Rozhkova, A. S. Dotsenko, I. N. Zorov, A. P. Sinitsyn, M. D. Davari and U. Schwaneberg, KnowVolution of a GH5 cellulase from *Penicillium verruculosum* to improve thermal stability for biomass degradation, *ACS Sustain. Chem. Eng.*, 2020, **8**, 33, 12388-12399.

30. C. Novoa, G. V. Dhoke, D. M. Mate, R. Martínez, T. Haarmann, M. Schreiter, J. Eidner, R. Schwerdtfeger, P. Lorenz, M. D. Davari, F. Jakob and U. Schwaneberg, KnowVolution of a fungal laccase toward alkaline pH, *ChemBioChem*, 2019, **20**, 11, 1458-1466.

31. A.-M. Wallraf, H. Liu, L. Zhu, G. Khalfallah, C. Simons, H. Alibiglou, M. D. Davari and U. Schwaneberg, A loop engineering strategy improves laccase lcc2 activity in ionic liquid and aqueous solution, *Green Chem.*, 2018, **20**, 12, 2801-2812.

32. K. Rübsam, B. Stomps, A. Böker, F. Jakob and U. Schwaneberg, Anchor peptides: A green and versatile method for polypropylene functionalization, *Polymer*, 2017, **116**, 124-132.

33. S. Dedisch, A. Wiens, M. D. Davari, D. Söder, C. Rodriguez-Emmenegger, F. Jakob and U. Schwaneberg, Matter-tag: A universal immobilization platform for enzymes on polymers, metals, and silicon-based materials, *Biotechnol. Bioeng.*, 2020, **117**, 1, 49-61.

34. Y. Lu, F. Bourdeaux, B. Nian, P. Manimaran, B. Verma, M. Rommerskirchen, S. Bold, L. Zhu, Y. Ji, J. H. Schleifenbaum and U. Schwaneberg, Engineered material-binding peptide empowers biocatalysis in stainless steel flow reactors for phosphate recovery, *Chem.*, 2025, **11**, 5.

35. S. Strnad and L.F. Zemljič, Cellulose–chitosan functional biocomposites, *Polymers*, 2023, **15**, 425.

36. Y. Li, L. Cai, H. Chen, Q. Gao and J. Li, Preparation and properties of soybean protein adhesive modified by chitosan/tannic-silver nanocomposite, *Wood Mater. Sci. Eng.,* 2023, **18**, 3, 852-859.

37. J. Wang, Z. Liang, Q. Yan, X. Bi, S. Bian, S. Luo, W. Yu, S. Zhang and S. Chen, Double-network soy protein adhesives with enhanced water retention and bonding strength, *Chem. Eur. J.*, 2025, **31**, 61, e02568.

38. O.I.V. Luotonen, L.G. Greca, G. Nyström, J. Guo, J.J. Richardson, O.J. Rojas and B.L. Tardy, Benchmarking supramolecular adhesive behavior of nanocelluloses, cellulose derivatives and proteins. *Carbohydr. Polym.*, 2022, **292**, 119681.

39. K. J. De France, N. Kummer, S. Campioni and G. Nyström, Phase behavior, self-assembly, and adhesive potential of cellulose nanocrystal–bovine serum albumin amyloid composites, *ACS Appl. Mater. Interfaces*, 2023, **15**, 1, 1958-1968.

40. H. Li, R. Fan, F. Zhang, Z. Cui, J. Li, Y. Cai, L. Kang, X. Zhan, J. Li, D. Tian, A spider-silk-inspired soybean protein adhesive with high-strength and mildew-resistant via synergistic effect of MXene nanosheets and chitosan, *Ind. Crops Prod.*, 2023, **193**, 116252.

41. J. P. de Mesquita, C. L. Donnici, I. F. Teixeira and F. V. Pereira, Bio-based nanocomposites obtained through covalent linkage between chitosan and cellulose nanocrystals, *Carbohydr. Polym.*, 2012, **90**, 1, 210-217.

View Article Online
DOI: 10.1039/D6GC00733C

42. H. Xie, Y. Wang, K. Ouyang, L. Zhang, J. Hu, S. Huang, W. Sun, P. Zhang, H. Xiong and Q. Zhao, Development of chitosan/rice protein hydrolysates/ZnO nanoparticles films reinforced with cellulose nanocrystals, *Int. J. Biol. Macromol.*, 2023, **236**, 123877.

43. M. R. Kuddus, F. Rumi, M. Tsutsumi, R. Takahashi, M. Yamano, M. Kamiya, T. Kikukawa, M. Demura and T. Aizawa, Expression, purification and characterization of the recombinant cysteine-rich antimicrobial peptide snakin-1 in *Pichia pastoris*, *Protein Expr. Purif.*, 2016, **122**, 15-22.

44. S. Franks, Strength and integrity: The basics of medical package testing, *Pharm. Med. Packag. News*, 2002, **28**, 34.

45. A. K. Rana, E. Frollini and V. K. Thakur, Cellulose nanocrystals: Pretreatments, preparation strategies, and surface functionalization, *Int. J. Biol. Macromol.*, 2021, **182**, 1554-1581.

46. T. Todorovic, E. Norström, F. Khabbaz, J. Brücher, E. Malmström and L. Fogelström, A fully bio-based wood adhesive valorising hemicellulose-rich sidestreams from the pulp industry, *Green Chem.*, 2021, **23**, 9, 3322-3333.

47. A. K. Patel, Chitosan: Emergence as potent candidate for green adhesive market, *Biochem. Eng. J.*, 2015, **102**, 74-81.

48. Y. Luo, J. Wang, T. Lv, H. Wang, H. Zhou, L. Ma, Y. Zhang and H. Dai, Chitosan particles modulate the properties of cellulose nanocrystals through interparticle interactions: Effect of concentration. *Int. J. Biol. Macromol.*, 2023, **240**, 124500.

49. A. Griffo, B. J. M. Rooijakkers, H. Hähl, K. Jacobs, M. B. Linder and P. Laaksonen, Binding forces of cellulose binding modules on cellulosic nanomaterials. *Biomacromolecules*, 2019, **20**, 2, 769-777.

50. Kusmono, M. W. Wildan and F. I. Lubis, Fabrication and characterization of chitosan/cellulose nanocrystal/glycerol bio-composite films, *Polymers*, 2021, **13**, 7.

51. C. D. Tran, S. Duri, A. Delneri and M. Franko, Chitosan-cellulose composite materials: Preparation, characterization and application for removal of microcystin, *J. Hazard. Mater.*, 2013, **252-253**, 355-366.

52. M. Fernandes Queiroz, K. R. Melo, D. A. Sabry, G. L. Sassaki and H. A. Rocha, Does the use of chitosan contribute to oxalate kidney stone formation?, *Mar. Drugs*, 2015, **13**, 1, 141-158.

53. Y. Luo, J. Wang, T. Lv, H. Wang, H. Zhou, L. Ma, Y. Zhang and H. Dai, Chitosan particles modulate the properties of cellulose nanocrystals through interparticle interactions: Effect of concentration, *Int. J. Biol. Macromol.*, 2023, **240**, 124500.

54. M. G. Aguayo, A. Fernández Pérez, G. Reyes, C. Oviedo, W. Gacitúa, R. Gonzalez and O. Uyarte, Isolation and characterization of cellulose nanocrystals from rejected fibers originated in the kraft pulping process, *Polymers*, 2018, **10**, 10.

55. J. K. Ogunjobi, A. I. Adewale and S. A. Adeyemi, Cellulose nanocrystals from Siam weed: Synthesis and physicochemical characterization, *Heliyon*, 2023, **9**, 1, e13104.

56. M. Yadav, K. Behera, Y. H. Chang and F. C. Chiu, Cellulose Nanocrystal Reinforced Chitosan Based UV Barrier Composite Films for Sustainable Packaging, *Polymers (Basel)*, 2020, **12**, 1.

57. D. Idamayanti, D. Taufik, M. R. G. Nadi, N. L. W. Septiani, A. Rochliadi, B. S. Purwasasmita, B. Yuliarto and A. Nuruddin, The cellulose nanocrystal (CNC)-reinforced chitosan composite as a potential substrate for flexible hard carbon anode in sodium-ion battery, *Cellulose*, 2023, **30**, 12, 7713-7728.

58. J. Yang, J. Duan, N. Na, B. Lindman, H. Edlund and M. Norgren, Spherical nanocomposite particles prepared from mixed cellulose–chitosan solutions, *Cellulose*, 2016, **23**, 3105-3115.

59. S. Siva Sangu, S. Chandra Bose Gopinath, M. F. Abdul Shukur and M. S. Mohamed Saheed, An electrochemical approach for ultrasensitive detection of zearalenone in commodity using disposable screen-printed electrode coated with mxene/chitosan film, *BioNanoScience*, 2022, **12**, 3, 814-823.

60. P.C. Li, G.M. Liao, D.S.R. Kumar, C.M. Shih, C.C. Yang, D.M. Wang and S. Lue, Fabrication and characterization of chitosan nanoparticle-incorporated quaternized poly(vinyl alcohol) composite membranes as solid electrolytes for direct methanol alkaline fuel cells, *Electrochim. Acta*, 2015, **187**.

61. S. Barazzouk and C. Daneault, Amino acid and peptide immobilization on oxidized nanocellulose: Spectroscopic characterization, *Nanomaterials*, 2012, **2**, 2, 187-205.

62. S. Rizal, E. B. Yahya, H. P. S. Abdul Khalil, C. K. Abdullah, M. Marwan, I. Ikramullah and U. Muksin, Preparation and characterization of nanocellulose/chitosan aerogel scaffolds using chemical-free approach, *Gels*, 2021, **7**, 4.

63. F. Ferrero and M. Periolatto, Antimicrobial finish of textiles by chitosan UV-curing, *J. Nanosci. Nanotechnol.*, 2012, **12**, 6, 4803-10.

64. J. Campos, P. Díaz-García, I. Montava, M. Bonet-Aracil and E. Bou-Belda, Chitosan pretreatment for cotton dyeing with black tea, *IOP Conf Ser: Mater. Sci. Eng.*, 2017, **254**, 11, 112001.

65. X. Wu, Y. Gao, H. Yao, K. Sun, R. Fan, X. Li, Y. An, Y. Lei and Y. Zhang, Flexible and transparent polymer/cellulose nanocrystal nanocomposites with high thermal conductivity for thermal management application, *J. Appl. Polym. Sci.*, 2020, **137**, 28, 48864.

66. E. Wittenberg, A. Meyer, S. Eggers and V. Abetz, Hydrogen bonding and thermoplastic elastomers – a nice couple with temperature-adjustable mechanical properties, *Soft Matter.*, 2018, **14**, 14, 2701-2711.

67. A. Baral and K. Basu, Supramolecular adhesives inspired by nature: Concept and applications, *Biomimetics*, 2025, **10**, 2.

68. Q. Zhang, C. Li, X. Du, H. Zhong, Z. He, P. Hong, Y. Li and Z. Jing, High strength, tough and self-healing chitosan-based nanocomposite hydrogels based on the synergistic effects of hydrogen bond and coordination bond, *J. Polym. Res.*, 2022, **29**, 8, 335.

69. V. M. R. Pires, P. M. M. Pereira, J. L. A. Brás, M. Correia, V. Cardoso, P. Bule, V. D. Alves, S. Najmudin, I. Venditto, L. M. A. Ferreira, M. J. Romão, A. L. Carvalho, C. M. G. A. Fontes and D. M. Prazeres, Stability and ligand promiscuity of type A carbohydrate-binding modules are illustrated by the structure of *Spirochaeta thermophila St* CBM64C, *J. Biol. Chem.*, 2017, **292**, 12, 4847-4860.

70. N. H. Halim, K. S. Lau, N. F. Jafri, N. A. Ghazali, R. Roslan, S. Zakaria, S. X. Chin and C. H. Chia, Cellulose nanocrystal-graft-polyacrylic acid /polyvinyl alcohol hydrogels: Physicochemical properties and swelling behavior, *Cellulose*, 2024, **31**, 10, 6263-6280.

View Article Online
DOI: 10.1039/D6GC00733C

71. L. Dong, W. Zhi, W. Li and J. Li, Parameters optimization for decontamination and fine physical regeneration pathways of polypropylene plastics from waste lunchboxes, *J. Hazard. Mater.*, 2024, **470**, 134247.

72. L. Bichler, E. Pinter, M. Jones, T. Koch, N. Krempl and V. Archodoulaki, Impacts of washing and deodorization treatment on packaging-sourced post-consumer polypropylene, *J. Mater. Cycles Waste Manag.*, 2024, **26**, 3824-3837.

73. Wang, C., H. Wang, and Y. Liu, Separation of aluminum and plastic by metallurgy method for recycling waste pharmaceutical blisters. *J. Clean Prod.*, 2015, **102**, 378-383.

74. C.-q. Wang, H. Wang, G.-h. Gu, J.-g. Fu and Y.-n. Liu, Kinetics and leaching behaviors of aluminum from pharmaceutical blisters in sodium hydroxide solution, *J. Cent. South Univ.*, 2015, **22**, 12, 4545-4550.

75. J. Nieminen, I. Anugwom, M. Kallioinen and M. Mänttäri, Green solvents in recovery of aluminium and plastic from waste pharmaceutical blister packaging, *Waste Manag.*, 2020. **107**, 20-27.

76. M. Muqaddas, I. Bibi, M. Atif, M. Asrar, R. Imtiaz, H. Tariq, M. S. Gohar, K. T. Kubra, N. Aslam, Advances in debondable adhesives: A focus on pH-dependent reversible bonding technologies, *Polym. Rev.*, 2025, **65**, 4, 1011-1056.

77. A. Bardow, J. Pérez-Ramírez, S. Sala and L. Vaccaro, Measuring green chemistry: methods, models, and metrics, *Green Chem*, 2024, **26**, 22, 11016-11018.

78. D. Kim, Y. Park and M.S. Kwon, Debonding-on-demand adhesives for recycling and reusing of electronic device, *Mater. Horiz.*, 2025, **12**, 14, 4934-4939.

79. D.V. Srinivasan and S. Idapalapati, Review of debonding techniques in adhesively bonded composite structures for sustainability, *Sustain. Mater. Technol.*, 2021. **30**, e00345.

80. P. Li, X. Wu, H. Zhang, C. Tan, X. Sha, N. Li, F. Zeng, Z. Wang, Research progress on controlled disassembly adhesives, *Prog. Org. Coat.*, 2025, **208**, 109520.

81. X. Lian, Y. Li, P. Li, Y. Jin, X. Zhao, J. Li, D. Kong, S. Zhao, S. Xiang, F. Fu, X. Liu, Wood-inspired dynamic covalent cross-linking network for ultrahigh adhesion strength, desired weather resistance, and closed-loop recycling adhesives, *ACS Appl. Mater. Interfaces*, 2025, **17**, 33, 47707-47718.

82. Z. Liu, Y. Tang, Y. Chen, Z. Lu and Z. Rui, Dynamic covalent adhesives and their applications: Current progress and future perspectives, *Chem. Eng. J.*, 2024, **497**, 154710.

83. M. Inada, T. Horii, T. Fujie, T. Nakanishi, T. Asahi and K. Saito, Debonding-on-demand adhesives based on photo-reversible cycloaddition reactions, *Mater. Adv.*, 2023, **4,** 5, 1289-1296.

Data availability

View Article Online
DOI: 10.1039/D6GC00733C

The data supporting the findings of this study are available within the article and its Electronic Supplementary Information (ESI).